The *BCL-6* proto-oncogene controls germinal-centre formation and Th2-type inflammation

Bihui H. Ye[1], Giorgio Cattoretti[1], Qiong Shen[1], Jiandong Zhang[1], Nicola Hawe[4], Rick de Waard[3], Cynthia Leung[3], Mahyar Nouri-Shirazi[3], Attilio Orazi[6], R.S.K. Chaganti[5], Paul Rothman[3], Alan M. Stall[3], Pier-Paolo Pandolfi[4] & Riccardo Dalla-Favera[1–2]

Structural alterations of the promoter region of the *BCL-6* proto-oncogene represent the most frequent genetic alteration associated with non-Hodgkin lymphoma, a malignancy often deriving from germinal-centre B cells. The *BCL-6* gene encodes a zinc-finger transcriptional repressor normally expressed in both B cells and CD4+ T cells within germinal centres, but its precise function is unknown. We show that mice deficient in BCL-6 displayed normal B-cell, T-cell and lymphoid-organ development but have a selective defect in T-cell-dependent antibody responses. This defect included a complete lack of affinity maturation and was due to the inability of follicular B cells to proliferate and form germinal centres. In addition, BCL-6-deficient mice developed an inflammatory response in multiple organs characterized by infiltrations of eosinophils and IgE-bearing B lymphocytes typical of a Th2-mediated hyperimmune response. Thus, BCL-6 functions as a transcriptional switch that controls germinal centre formation and may also modulate specific T-cell-mediated responses. Altered expression of BCL-6 in lymphoma represents a deregulation of the pathway normally leading to B cell proliferation and germinal centre formation.

The *BCL-6* proto-oncogene was identified by virtue of its involvement in chromosomal translocations in diffuse large cell lymphoma (DLCL), the most common form of non-Hodgkin lymphoma (NHL)[1–6]. Subsequent studies have demonstrated that rearrangements of the *BCL-6* gene can be found in 30–40% of DLCLs and in a minority (5–10%) of follicular lymphomas (FL)[7–9]. These rearrangements juxtapose heterologous promoters, derived from other chromosomes, to the *BCL-6* coding domain, causing its deregulated expression by a mechanism called promoter substitution[10]. The 5' non-coding region of the *BCL-6* gene can also be altered by somatic point mutations that are detectable, independent of rearrangements, in approximately 70% of DLCLs, in 45% of FLs and in AIDS-associated NHL[11,12]. Taken together, rearrangements and mutations of the *BCL-6* promoter region represent the most frequent genetic alteration in human B-cell malignancies, suggesting that they may be important for tumorigenesis[13].

The *BCL-6* gene encodes a nuclear phosphoprotein characterized by six *Kruppel*-type C-terminal zinc-finger (ZF) motifs[2,5,6] that have been shown to recognize specific DNA sequences *in vitro*[14,15], and by an N-terminal POZ motif[5,16] shared by various ZF molecules, including the *Drosophila* developmental regulators *Tramtrack* and *Broad-Complex*[17,18], the human KUP[19], ZID[20] and PLZF[21] proteins, by some proteins of POX viruses[22] and by the actin-binding *Drosophila* oocyte protein, *Kelch*[23]. BCL-6 functions as a potent transcriptional repressor of promoters linked to its DNA target sequence[14,15,24]. Recent results suggest that BCL-6 can bind the Stat-6 DNA binding site and repress Stat-6-mediated IL-4 signaling (Chang, C.-C. *et al.*, pers. comm.).

BCL-6 mRNA is found at low abundance in multiple tissues; high levels of protein expression are found only in the lymphoid system[25,26]. In the B-cell lineage, BCL-6 protein is found only in B cells within germinal centres (GC), but not in pre-B cells or in differentiated progenies such as plasma cells[25–27]. In the T lineage, BCL-6 protein is detectable in cortical thymocytes and in $CD4^+$ T cells within the GC in addition to those scattered in the perifollicular area[25–28].

This study elucidates the biological role of BCL-6 by analysing the phenotype of mice in which BCL-6 has been inactivated. It shows that BCL-6 is necessary for the development of GC and a normal T-cell-dependent antibody response. In addition, BCL-6-deficient mice display a characteristic inflammatory response, which implicates BCL-6 in the control of Th2-mediated responses. Thus, our results identify *BCL-6* as a gene important in regulating both B- and T-cell responses and have direct implications for the role of deregulated BCL-6 expression in lymphomagenesis.

Disruption of the *BCL-6* gene in the mouse germ-line

Disruption of the *BCL-6* gene was obtained by homologous recombination in embryonic stem (ES) cells using two targeting vectors. The first generated a truncated *BCL-6* allele (*BCL-6Δ*) lacking sequence (exon 8-9) coding the COOH-terminal half of the BCL-6 protein corresponding to four of six zinc-fingers of its DNA-binding domain (Fig. 1*a*). This allele encodes a truncated protein (BCL-6ΔZF) that cannot bind DNA (not shown) and localizes mainly in the cytoplasm (Fig. 6), consistent with the observation that DNA binding and nuclear localization are dependent upon the COOH-

Departments of [1]Pathology, [2]Genetics and Development, and [3]Microbiology, Columbia University, New York, New York 10032, USA. Department of Human Genetics, [4]Molecular Biology and [5]Cell Biology Programs, Memorial Sloan-Kettering Cancer Center, New York, New York 10021, USA. [6]Department of Pathology and Laboratory Medicine, Indiana University School of Medicine, Indianapolis, Indiana 46202, USA. Correspondence should be addressed to R.D.-F; e-mail rd10@columbia.edu

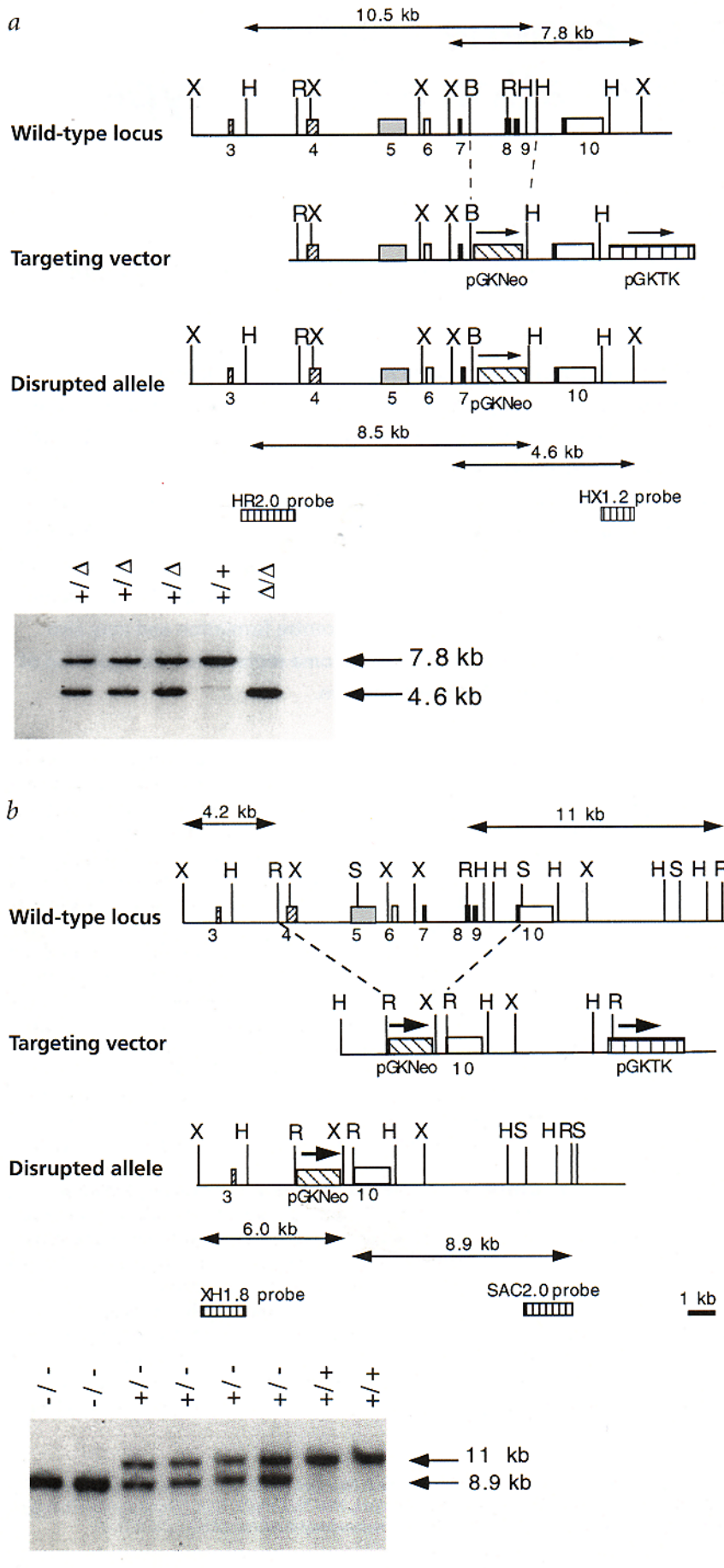

Fig. 1 Targeted disruption of the *BCL-6* gene in the mouse germ line. ***a,*** Schematic representation of the mouse *BCL-6* locus before (top) and after (bottom) homologous recombination with the targeting vector (middle) generating the *BCL-6*$^{\Delta}$ allele. Expected restriction fragments and probes used for Southern blot analysis are also indicated. *BCL-6* exons are indicated by boxes (slashed: POZ coding domain; dotted: region between POZ and zinc fingers; filled: zinc finger domain; empty: non-coding exons). The *BCL-6* coding sequence was disrupted by insertion of a cassette containing the neomycin-resistance gene under the control of the pGK promoter (for the positive selection of transfected cells) and the thymidine kinase (TK) gene also under the control of the pGK promoter (negative selection against random integration). Restriction sites: B, *Bgl*II; H, *Hin*dIII; R, *Eco*RI; X, *Xba*I. Below: Southern blot analysis of *Xba*I-digested tail DNA from offspring generated by mating *BCL-6*$^{+/\Delta}$ mice showing the wild-type 7.8-kb and the mutated 4.6-kb fragments. ***b,*** Schematic representation of the mouse *BCL-6* locus before (top) and after (bottom) homologous recombination with the targeting vector (middle), generating the *BCL-6*$^{-}$ allele. Southern blot analysis of *Eco*RI-digested tail DNA of offsprings generated by mating *BCL-6*$^{+/\Delta}$ mice shows the wild-type 11-kb and the mutated 8.9-kb fragments.

terminal half of the BCL-6 molecule[29]. The second construct was targeted to *BCL-6* exons 4–10, corresponding to virtually the entire (92.5%) *BCL-6* coding domain. It produced a BCL-6 'null' allele with no coding capacity (*BCL-6*$^{-}$) (Fig. 1*b*; see also Fig. 5). Genotypic analysis of the offspring (Fig. 1) indicated that normal (*BCL-6*$^{+/+}$), heterozygous (*BCL-6*$^{+/\Delta}$ or *BCL*$^{+/-}$) and homozygous (*BCL-6*$^{\Delta/\Delta}$ or *BCL-6*$^{-/-}$) animals were born at expected mendelian frequencies (not shown). The offspring generated from four independent ES clones (3 *BCL-6*$^{\Delta}$; 1 *BCL-6*$^{-}$) indicated that both types of heterozygous animals were phenotypically indistinguishable from wild-type, while homozygous *BCL-6*$^{\Delta/\Delta}$ and $^{-/-}$ mice displayed an identical pathologic phenotype (see below). Thus, similar to the fully-deleted *BCL-6*$^{-}$ allele, the truncated *BCL-6*$^{\Delta}$ gene is functionally 'null'.

Bacterial infections in BCL-6 null mice

At birth, all heterozygous and homozygous mice were indistinguishable from wild-type littermates in morphology and weight. However, while wild-type and heterozygous mice remained indistinguishable during a six-month follow-up, the growth of *BCL-6*$^{\Delta/\Delta}$ or *BCL-6*$^{-/-}$ mice derived from all four ES lines was significantly retarded (*BCL-6*$^{\Delta/\Delta}$: 51.7 ±5.3 % the weight of wild-type age-matched littermates; *BCL-6*$^{-/-}$: 42.8% ± 19 %). No gross developmental abnormalities were noted and the weights of

most organs were comparable in wild-type, heterozygous and BCL-6 null mice after normalization for body weight; the spleen weight was more variable in BCL-6 null mice showing hyperplasia due to infiltration by non-lymphoid cells in some animals (see below) and occasional hypoplasia in very young mice (< 2 weeks old); the thymus was smaller in some mice, particularly in those with early infections (see below). As no specific developmental abnormality was detectable at birth, growth retardation was attributed to the infectious and inflammatory diseases developed later by these animals (see below), and in particular to oesophagitis, which may impair their capability to intake food.

Approximately half of the BCL-6 null mice (*BCL-6*$^{\Delta/\Delta}$, 30/70; *BCL-6*$^{-/-}$, 8/18), but none of the wild-type (0/50) or heterozygous (0/27) mice, displayed infections within the first three months of life. These infections had a variable clinical course ranging from subclinical (that is, detectable at autopsy) to lethal, and they most frequently involved the oesophagus, but also various other mucosal sites in the upper respiratory and digestive tracts (orbit, ear and nose) as well as the lung. Pathologic examination of these lesions showed infiltrates of granulocytes and monocytes occasionally leading to frank abscesses. Histochemical staining and testing for anti-viral antibodies (see Methods) showed that these infections were due to bacteria (Fig. 2); infections were explained by the impaired antigen-specific antibody response of BCL-6 null mice (see below).

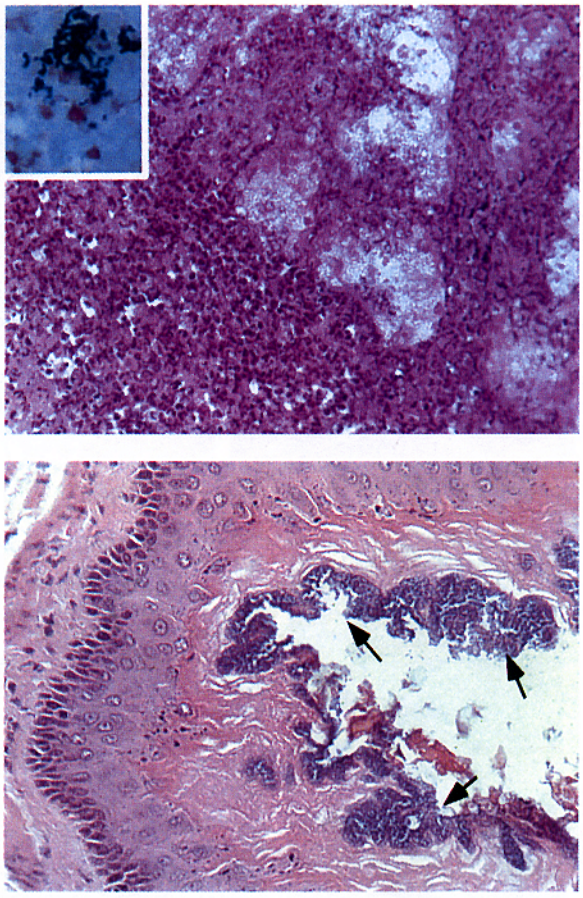

Fig. 2 Infections in *BCL-6* null mice. Acute suppurative inflammation of a lacrimal gland (top). The gland structure is effaced by numerous polymorphonuclear leucocytes and local abscess formation. In the inset, bacterial clumps are stained positive with Gram stain. Oesophageal colonization by bacterial colonies (bottom). Thick colonies of bacteria (arrows) coat the oesophageal surface. Note the absence of reactive inflammation in the epithelium and submucosa.

BCL-6 null mice develop a Th2-type inflammatory disease

A second disorder of BCL-6 homozygous mutant mice was represented by a systemic inflammatory disease involving multiple organs most frequently including the myocardium, spleen, gut, liver and skin. Prominent signs of inflammation in one or more organs were detectable in 61 of 70 (87%) *BCL*$^{\Delta/\Delta}$ mice and in 14 of 18 (77%) *BCL-6*$^{-/-}$ mice (features were macroscopically and microscopically indistinguishable between two types of mice), but in none of the heterozygous (0/27) or wild-type (0/50) animals. The pathologic picture was characterized by prominent eosinophilic infiltrates (Fig. 3*a*), which were first detectable as intraepithelial infiltrates in the gut of young animals at three months. These infiltrates were often accompanied or followed by a lympho-monocytic component (Fig. 3*a*). The presence of eosinophilic infiltrates in lung, heart and mediastinal lymph nodes was invariably associated with a particular mouse disease of the lung, called acidophilic macrophage pneumonia[30], and characterized by the infiltration of macrophages filled by degradation products of eosinophils (Fig. 3*a*). In these animals, the bone marrow showed a modest increase in eosinophilic precursors, while no peripheral eosinophilia was observed. The involved organs tested negative for bacteria and parasites and did not show pathologic signs of viral infection (data not shown; see Methods).

Since BCL-6 is not expressed in eosinophils in humans[25] and mice (Cattoretti, G. *et al.*, pers. comm.), their altered regulation suggested a Th2-mediated inflammatory reaction[31]. To examine this possibility, we investigated whether BCL-6 null mice also had abnormal distributions of IgG_1 and IgE, features also typical of Th2-mediated responses[31]. By immunohistochemical anaysis, a dramatic increase in IgE in eosinophil-absorbed form was detected in the gut (Fig. 3*b*) and a significant number of IgE-expressing B cells was detectable in various organs including the spleen and liver in *BCL-6*$^{\Delta/\Delta}$ and $^{-/-}$ mice but not in control littermates (Fig. 3*b*). Markedly increased number of IgG1-bearing plasmacytoid cells, identified by double-staining with antibodies for IgG1 and the mature B-cell marker syndecan, was also detectable in the perifollicular areas of the spleen of BCL-6 null mice (Fig. 3*b*). The number of IgG2a- and IgG2b-positive cells was also increased, although less dramatically. No alteration in the expression of other immunoglobulin (Ig) isotypes (IgA and IgG3) was detectable by immunohistochemical analysis on the same tissue sections. Taken together, the organ infiltrations by eosinophils and an increase in IgG1- and IgE-bearing B cells are consistent with a Th2-mediated inflammatory response in BCL-6 null mice.

Normal B and T cell populations and lymphoid organ development in BCL-6 null mice

The presence of bacterial infections and inflammatory disease as well as the fact that *BCL-6* is normally expressed at high levels in lymphoid cells[25] prompted a detailed investigation of the development of the lymphoid tissues in the *BCL-6* mutant mice. Upon histologic examination, both *BCL-6*$^{\Delta/\Delta}$ and $^{-/-}$ mice displayed normal development of the bone marrow, spleen, thymus, lymph nodes and Peyer's patches (not shown).

Flow cytometric analysis of bone marrow, spleen, thymus, lymph nodes and peritoneal cavity cells indicated that BCL-6 null mice had normal numbers and distributions of B cells (pro-B: IgM^-, $B220^{lo}$, $CD43^+$; pre-B: IgM^-, $B220^+$, $CD43^-$; immature B: IgM^+, IgD^+, $CD23^+$, $B220^{hi}$, $CD5^{+/-}$, $CD43^{+/-}$; resting mature B: IgM^{hi}, IgD^{lo}, $CD23^-$, $B220^{hi}$, $CD5^{+/-}$, $CD43^{+/-}$; B1 cells: IgM^+, IgD^+, $B220^+$, $CD5^+$, Mac-1^+) as well as T cells (pro-thymocytes: $CD3^{lo}$, $CD4^-$, $CD8^-$; cortical thymocytes: $CD3^+$, $CD4^+$, $CD8^+$, peripheral T cells: $CD3^+$, $CD4^{+/-}$, $CD8^{-/+}$) (not shown; see Methods for details on the characterization of lymphoid subpopulations)[32,33]. These results show that BCL-6 is not required for lym-

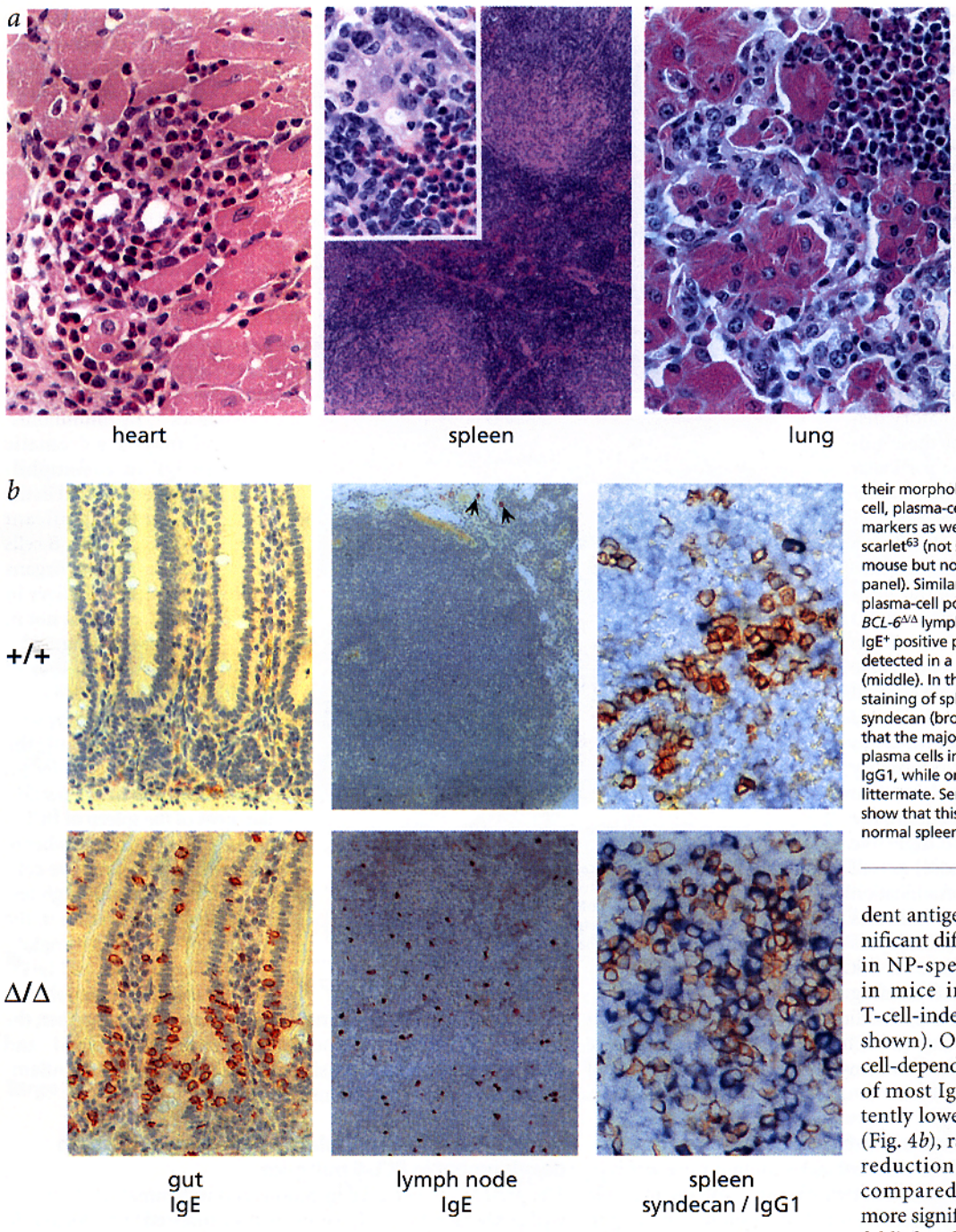

Fig. 3 Inflammatory disease in BCL-6 null mice. ***a,*** In the heart section, eosinophils infiltrate the interstitial space between myocytes in an early cardiac lesion (left panel). At low power, the spleen shows multinodular lesions in the white and red pulp (middle); these lesions are composed of eosinophils, monocytes and multinucleated giant cells (inset). In lung, collections of eosinophils in the interstitium are associated with intra-alveolar macrophages filled with Charcot-Leyden type crystals (right). ***b,*** IgE staining of gut (ileum) sections shows intraepithelial IgE$^+$ eosinophils [identified by their morphology, negativity for T-cell, B-cell, plasma-cell, and neutrophilic markers as well as staining with Biebrich scarlet[63] (not shown)] in the *BCL-6*$^{\Delta/\Delta}$ mouse but not in the $^{+/+}$ littermate (left panel). Similarly, an abundant IgE$^+$ plasma-cell population is detected in the *BCL-6*$^{\Delta/\Delta}$ lymph node, while only isolated IgE$^+$ positive plasma cells (arrows) are detected in a normal lymph node (middle). In the right panel, double staining of spleen sections with anti-syndecan (brown) and IgG1 (blue) shows that the majority of syndecan-positive plasma cells in *BCL-6*$^{\Delta/\Delta}$ mice co-express IgG1, while only a few do in the littermate. Serial sections stained for IgM show that this isotype is prevalent in a normal spleen (not shown).

phoid-organ development or for the normal differentiation and expansion of the B and T lineages.

Reduced antigen-specific T-cell-dependent Ig response and lack of affinity maturation in BCL-6 null mice

We analysed the ability of BCL-6 null mice to produce antibodies and to mount an antigen specific immune response. Basal serum levels of most Ig subtypes were modestly decreased in naive healthy BCL-6 null mice (Fig. 4*a*). The presence of all Ig isotypes in serum and in tissues (immunohistochemical analysis using anti-IgA, IgG1, IgG2a, IgG2b, IgG3 and IgE antibodies; not shown) suggested that these mice were able to undergo Ig isotype switching. In order to directly assess their ability to mount an antigen-specific antibody response, mice were immunized with either a T-cell-independent (NP-Ficoll) antigen or a T-cell-dependent antigen (NP-KLH). No significant difference was detectable in NP-specific Ig serum levels in mice immunized with the T-cell-independent antigen (not shown). On the contrary, the T-cell-dependent antibody response of most Ig isotypes was consistently lower in BCL-6 null mice (Fig. 4*b*), ranging from a modest reduction in IgM level (2-fold compared with wild-type) to more significant decreases (4–20-fold) for all IgG subtypes. Thus, the lack of a functional BCL-6 molecule caused a selective deficiency in T-cell-dependent antibody responses.

Affinity maturation is thought to be associated with the development of GC[34,35]. To determine whether affinity maturation takes place in BCL-6 null mice, we hyperimmunized wild-type and *BCL-6*$^{\Delta/\Delta}$ mice with NP-KLH and analysed the serum for the presence of high affinity antibodies (that is, those able to bind to a low haptenated protein, NP_3-BSA). The results demonstrate that while the class-switched IgG1 anti-NP specific antibodies in wild-type mice showed progressive affinity maturation in the secondary (2°) and tertiary (3°) responses, there is no detectable maturation in the BCL-6 null mice even following a third immunization (Fig. 4*c*). Thus, while the absence of BCL-6 results in a partial reduction in the IgG response, it leads to a complete lack of affinity maturation.

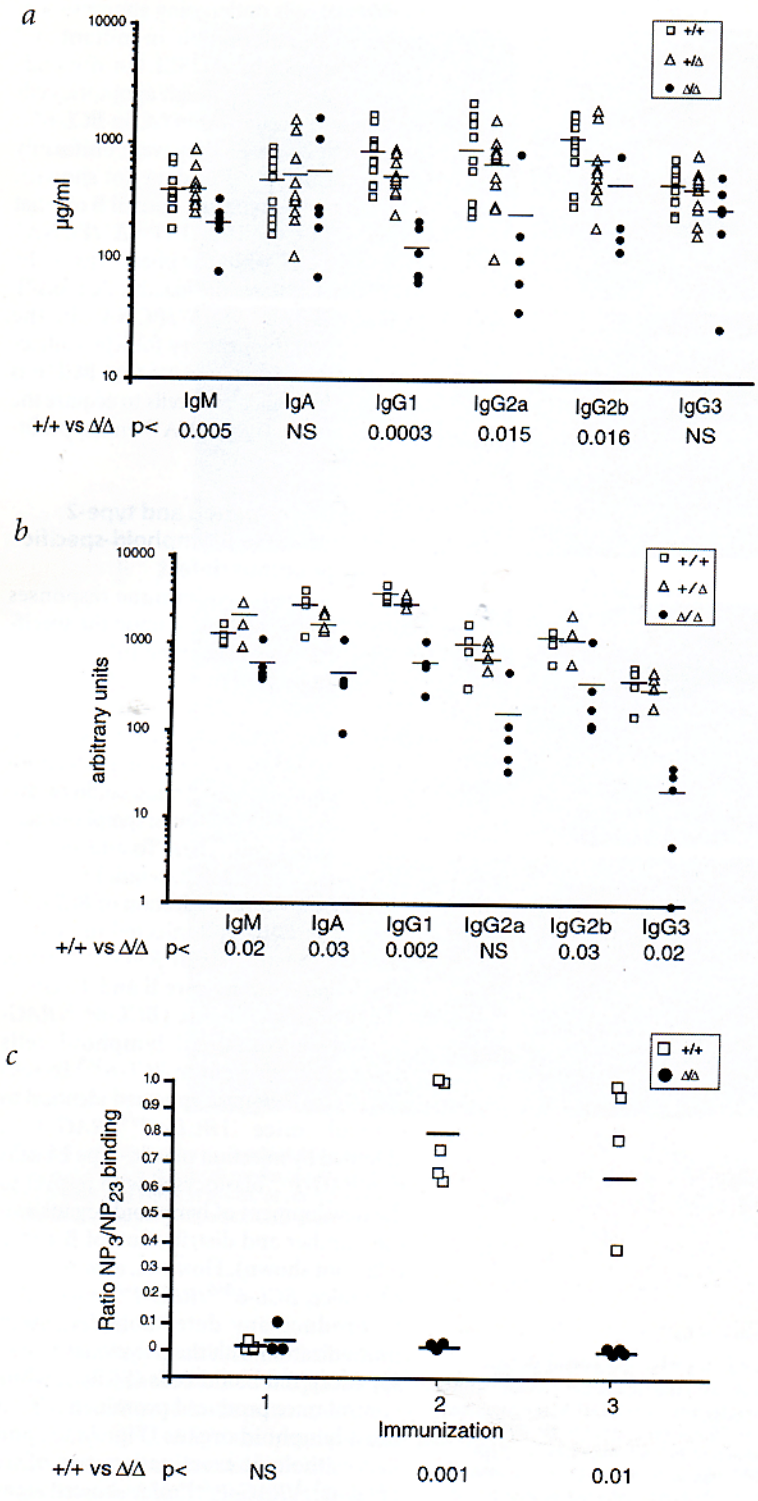

Fig. 4 Serum antibody levels in BCL-6 null mice. ***a,*** Resting serum antibody levels in the BCL-6 null mice. Serum samples were collected from 11–13-week-old mice and analysed by ELISA. *P*-values derived by Student's T test on the group means (indicated as short horizontal bars) of wild-type versus homozygous groups are given below each subclass in the graph. ***b,*** Reduced antigen-specific antibody responses in BCL-6 null mice. A litter of 11-week-old mice were immunized with NP-KLH and sacrificed 11 days later for immunohistological (Fig. 5) and ELISA analysis. The NP-specific titers for each subclass are relative. ***c,*** Lack of affinity maturation in BCL-6 null mice. Sibling wild-type or *BCL-6*$^{\Delta/\Delta}$ mice were immunized with NP-KLH on days 0, 21 and 42 and bled 5 days after each immunization. Sera were tested for the binding of NP-specific IgG1 antibodies to NP_3-BSA and NP_{23}-BSA coated plates. Higher NP_3/ NP_{23} binding ratios indicate the presence of higher-avidity (affinity-matured) antibodies.

Lack of germinal centre formation in BCL-6 null mice

Antibody response to T-dependent antigen is largely dependent on the ability of the B cell to undergo clonal expansion and affinity maturation within GC, while T-independent responses are typically GC-independent[34,35]. Thus, the reduced antigen-specific Ig response of BCL-6 null mice prompted us to examine their ability to form GC. Morphologic examination as well as immunohistochemical staining for the GC B-cell marker peanut agglutinin[36] and for the BCL-6 protein showed that non-immunized *BCL-6*$^{\Delta/\Delta}$ and $^{-/-}$ mice had no spontaneously formed GC in the spleen, although these structures were readily detectable in age-matched wild-type littermates (Fig. 5, top panels; note the absence of BCL-6 protein in *BCL-6*$^{-/-}$ mice). Upon immunization with the T-dependent antigen, both types of BCL-6 null mice failed to form GC in the spleen, lymph nodes and Peyer's patches, while these structures developed normally in immunized heterozygous and wild-type littermates (Fig. 5, bottom panels; note the scattered expression of the truncated BCL-6ΔZF protein in *BCL-6*$^{\Delta/\Delta}$ mice). The architecture of the lymphoid organs in BCL-6$^-$ null mice indicated that primary follicles formed, including mantle and T cell zones, but appeared distinctly 'empty' of GC even after repeated immunizations (Fig. 5). The lack of GC formation in these mice is consistent with their impaired ability to mount an antigen-specific Ig response to T-dependent antigens and with their complete lack of affinity maturation (Fig. 4*b-c*).

Mechanism of germinal centre defect: follicular B cells fail to proliferate and differentiate into GC

We investigated the mechanism by which BCL-6 null mice fail to form GC, and in particular whether the defect was due to lack of proliferation, differentiation or increased death of B cells. Standard *in vitro* proliferation assays using purified spleen IgM$^+$ B cells and various combinations of mitogens and activators (LPS, IL-4 and CD40 ligand) did not identify any significant difference between BCL-6 null and control mice (not shown). However, these assays could not adequately inform on the proliferative response of BCL-6-expressing cells because cells corresponding to the GC fraction are quite rare among total splenic B cells (<5%; unpublished data, C.G.); in addition, BCL-6-expressing cells cannot be purified from BCL-6 null animals, since they lack GC markers.

To circumvent these problems, we exploited the fact that the truncated protein (BCL-6ΔZF) produced by the *BCL-6*$^{\Delta/\Delta}$ mice is recognized by an antiserum raised against the amino-terminal portion of BCL-6, and can therefore be used to track *in vivo* the fate and phenotype of cells in which *BCL-6* gene expression is induced. Initial studies, using double immunohistochemical staining for IgD and BCL-6, showed that the expression of these two molecules is mutually exclusive in B cells of wild-type mice (mantle zone B cells: IgD$^+$/BCL-6$^-$; GC B cells: IgD$^-$/BCL-6$^+$; ref. 25), while the same molecules are co-expressed in sparse cells in the primary follicles of *BCL-6*$^{\Delta/\Delta}$ mice (data not shown). Triple-immunofluorescent staining for BCL-

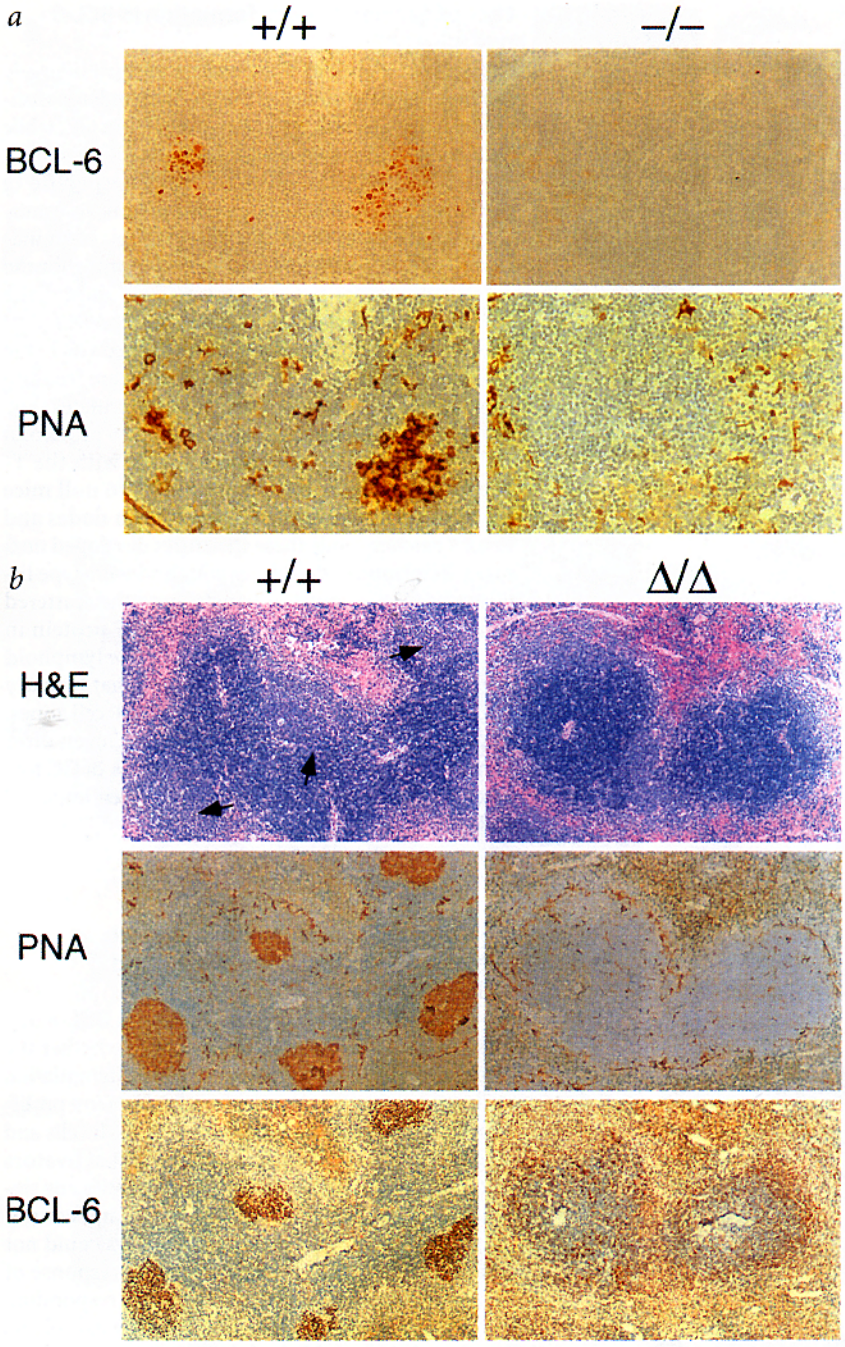

Fig. 5. Absence of GCs in the spleen of BCL-6 null mice immunized with a T cell-dependent antigen. ***a*** (four panels), serial spleen sections of BCL-$6^{+/+}$ and $^{-/-}$ mice stained with the GC marker peanut lectin (PNA) or the N3 anti-BCL-6 antiserum (BCL-6). ***b*** (six panels), serial spleen sections of NP-KLH immunized *BCL-*$6^{+/+}$, $^{+/\Delta}$ and $^{\Delta/\Delta}$ mice stained with hematoxylin/eosin (H&E), the GC marker peanut lectin (PNA), or the N3 anti-BCL-6 antiserum (BCL-6). The images show that the spleen of *BCL-*$6^{-/-}$ mice lack GC (PNA panels) as well as cells expressing BCL-6 (BCL-6 panels). The BCL-$6^{\Delta/\Delta}$ mice also lack GC (H&E and PNA panels) and contain cells expressing the truncated BCL-6ΔZF protein which are scattered as opposed to organized into GC as in *BCL-*$6^{+/+}$ mice. Analogous experiments performed on *BCL-*$6^{+/\Delta}$ mice showed that these mice are indistinguishable from wild-type controls.

6, the B-cell marker B220, and PNA (Fig. 6*a*) showed that BCL-6ΔZF-expressing B cells are dispersed in the follicular area of the spleen in *BCL-*$6^{\Delta/\Delta}$ mice and fail to express PNA. In addition, triple-immunofluorescent staining for BCL-6, the B-cell marker B220 and the proliferation-associated marker PCNA (Fig. 6*b*) showed that BCL-6ΔZF expressing B cells fail to express PCNA and therefore do not proliferate. In the same tissue sections, the number of cells undergoing apoptosis was found to be comparable in mutant and wild-type mice by an ISEL (in situ end-labeling) assay[37], although apoptotic cells appeared to cluster within GC in *BCL-*$6^{+/+}$ and $^{+/\Delta}$ mice, while they were uniformly dispersed in $^{\Delta/\Delta}$ mice (data not shown). Thus, the phenotype of a normal B cell that expresses BCL-6 is $IgD^-/PNA^+/PCNA^+$ within the GC, while the phenotype of the B cell that expresses the inactive BCL-6ΔZF protein is $IgD^+/PNA^-/PCNA^-$ in the periphery of the primary follicle. Collectively, these results indicate that BCL-6 is required for follicular B cells to acquire the GC phenotype (IgD^-/PNA^+) and to proliferate.

Lack of GC formation and type-2 inflammation as a lymphoid-specific cell-autonomous defect

Antibody-mediated immune responses within GC are dependent upon the specific cell-cell and paracrine interactions among various cell types, including B cells, T cells and follicular dendritic cells (FDC)[34]. Thus, the abnormalities detected in BCL-6 null mice, including infections and inflammatory infiltrates, could be due to defects in the function of lymphoid cells and/or other cell types. To address this issue, we generated BCL-6 null ES cells by high-dose neomycin selection of *BCL-*$6^{+/\Delta}$ ES cells *in vitro*, and injected these cells into the blastocysts of *RAG-*$1^{-/-}$ mice, which lack both mature B and T cells[38]. The resulting chimeric [*BCL-*$6^{\Delta/\Delta}$*/RAG-*$1^{-/-}$] mice contained lymphoid cells derived exclusively from *BCL-*$6^{\Delta/\Delta}$ ES cells (Fig. 7*a*). These mice appeared identical to control mice [*BCL-*$6^{+/+}$*/RAG-*$1^{-/-}$, obtained by injection of wild-type ES cells into *RAG-*$1^{-/-}$ blastocysts] with respect to the development of lymphoid organs and the number and distribution of B and T cells (not shown). However, as with *BCL-*$6^{\Delta/\Delta}$ mice, *BCL-*$6^{\Delta/\Delta}$*/RAG-*$1^{-/-}$ mice failed to produce any detectable GC upon immunization with the polyclonal activator sheep red blood cells (SRBC), while control mice produced prominent GC in most lymphoid organs (Fig. 7*b*). Upon histopathologic examination, two of six [*BCL-*$6^{\Delta/\Delta}$*/RAG-*$1^{-/-}$] mice showed signs of infection. Thus, the defect in GC formation in BCL-6-deficient mice is due to an intrinsic defect in the lymphoid compartment rather than to a defect in FDC or in soluble molecules produced by non-lymphoid cells. In addition, all [*BCL-*$6^{\Delta/\Delta}$*/RAG-*$1^{-/-}$] animals displayed intraepithelial eosinophilic infiltration of the gut, an early sign of Th2-type inflammation in *BCL-*$6^{-/-}$ animals. Thus, the abnormal inflammatory response also reflects a lymphoid-restricted defect consistent with the hypothesis that it may be due to the lack of BCL-6 function in lymphoid cells.

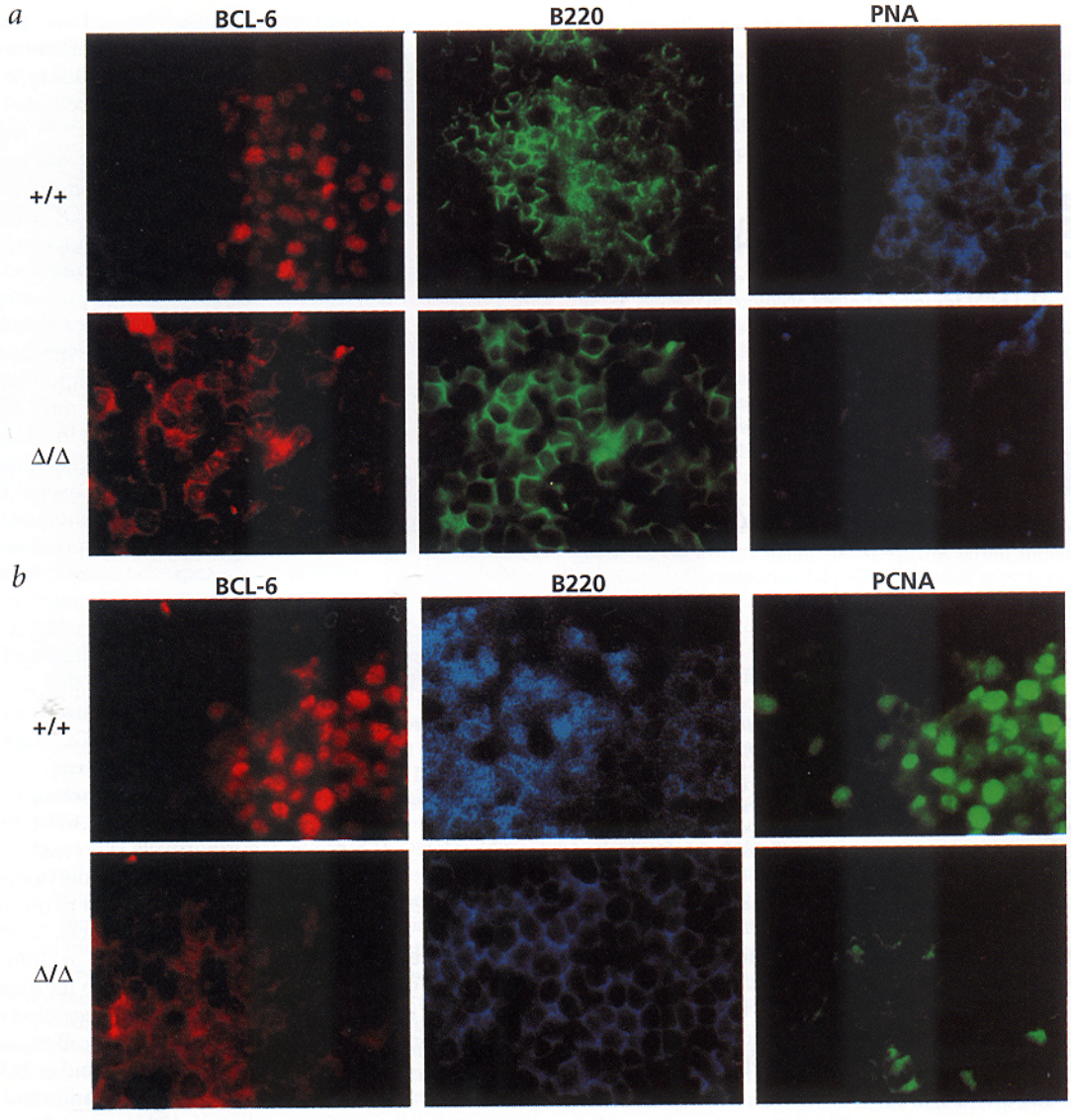

Fig. 6 B cells expressing the inactive BCL-6ΔZF protein fail to proliferate and acquire the germinal-centre phenotype. Spleen sections from *BCL-6*$^{+/+}$ and $^{\Delta/\Delta}$ mice stained for BCL-6, the B-cell marker B220 and the GC marker PNA **(a)** or the proliferation marker PCNA **(b).** The triple stainings show that most B cells express BCL-6, PNA and PCNA in the GC of control mice. Conversely, BCL-6ΔZF expressing B cells lack both PNA and PCNA expression in *BCL-6*$^{\Delta/\Delta}$ mice. Note the abnormal cellular distribution of the BCL-6ΔZF protein.

Discussion

In an attempt to understand the biological role of BCL-6 in lymphomagenesis we studied the phenotype of mice lacking a functional BCL-6 protein. In general, our results indicate that the main function of BCL-6 is in the lymphoid system as no primary pathologic feature was detectable in other tissues and all abnormalities were shown to be lymphoid-derived in the *RAG-1*$^{-/-}$ complementation study (Fig. 7). Based on the results obtained from the study of four independent BCL-6 null mouse lines, a lack of functional BCL-6 appears to lead to two major phenotypes: a systemic inflammatory disease, suggesting an unexpected role of BCL-6 in the control of Th2-dependent responses and a specific defect in GC formation, with direct implications for a role of BCL-6 in the pathogenesis of B-cell lymphoma.

Role of BCL-6 in Th2-type inflammation

The lymphoid-dependent phenotype of *RAG-1*$^{-/-}$/BCL-6$^{\Delta/\Delta}$ mice suggests that the inflammatory response of BCL-6 null mice is due to the function of BCL-6 in T and/or B cells. The pathologic features of the inflammatory disease, including organ infiltration by eosinophils and hyper-production of IgG1/IgE-bearing B cells, are typical of Th2-mediated hyper-responses[29]. Combined with the fact that BCL-6 is expressed in a subset of CD4$^+$ T cells, this phenotype suggests that BCL-6 modulates Th2 cell differentiation or function. Th2 cells are the critical regulators of allergic responses because they produce IL-4, which causes the preferential Ig switch of B cells toward the IgG1 and IgE isotypes[39,40], as well as IL-5, which leads to the stimulation of eosinophils[41]. In strong support of a role for BCL-6 in Th2 responses, we recently observed that BCL-6 can bind to the DNA target sequences of Stat-6, repress Stat-6-activated transcription and therefore cause the repression of Stat-6 mediated IL-4 responses (Chang *et al.*, manuscript in preparation), the main effectors of Th2 function and IgG1/IgE isotype switch in B cells[39,40]. Thus, it is possible that the inflammatory phenotype of BCL-6 null mice may be due to a lack of BCL-6 modulation of IL-4 signalling, which, in turn, would cause a

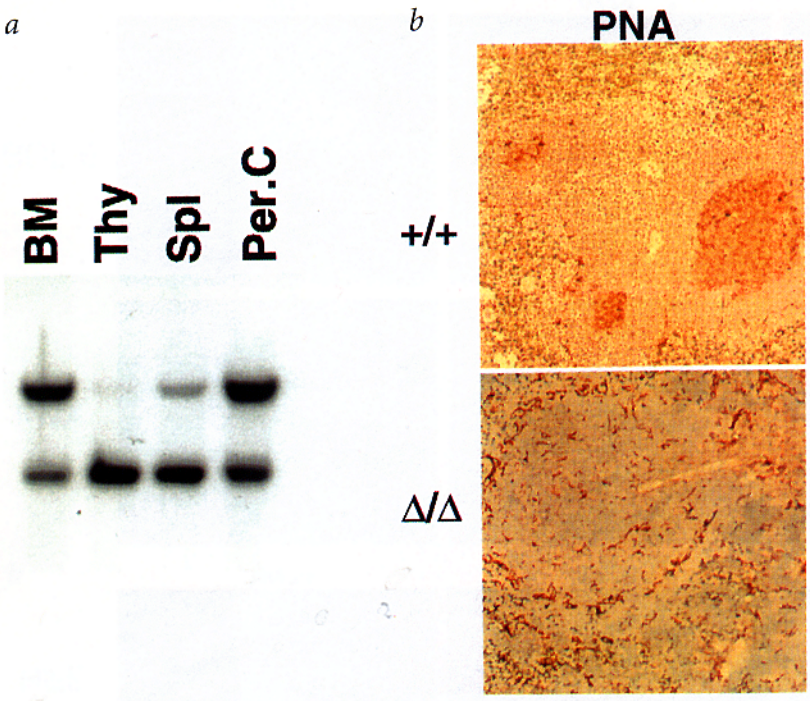

Fig. 7 Absence of GC in immunized *RAG-1*$^{-/-}$ mice reconstituted with *BCL-6*$^{\Delta/\Delta}$ ES cells. ***a***, Representative Southern-blot analysis of DNA derived from bone marrow (BM), thymus (Thy), spleen (Spl) and peritoneal cells (Per. C), showing variable presence of the disrupted *BCL-6* allele (4.6 kb) in a *BCL-6*$^{\Delta/\Delta}$*/RAG-1*$^{-/-}$ mouse. Note that the representation of the disrupted *BCL-6* allele is higher in lymphoid-rich organs (Thy and Spl) consistent with the reconstitution of the lymphoid compartment by *BCL-6*$^{\Delta/\Delta}$ ES cells. ***b***, To analyse GC formation, six *BCL-6*$^{\Delta/\Delta}$*/RAG-1*$^{-/-}$ chimeric animals (Δ/Δ) and three control (*BCL-6*$^{+/+}$*/RAG-1*$^{-/-}$, +/+) chimeras were immunized with SRBCs. Spleen sections of these mice stained with the GC marker PNA show that the spleen of *BCL-6*$^{\Delta/\Delta}$*/RAG-1*$^{-/-}$ mice lack GC.

hyper-response of Th2 cells to IL-4, leading to increased eosinophilic and IgG1/IgE B cell stimulation. Verification of this model and, in particular, of the role of BCL-6 in regulating Th2 lineage commitment and/or function, will require additional studies including the analysis of BCL-6 null T cells in Th-cell differentiation assays *in vivo* and *in vitro*[42].

Role of BCL-6 in T-cell-dependent antibody response

The presence of bacterial infections is explained by the defect in T-cell-dependent antibody response and the complete defect in affinity maturation in BCL-6 null mice. In fact, bacterial clearance is dependent on humoral immunity, and several human hereditary hypogammaglobulinemia or hyper-IgE syndromes are associated with a marked susceptibility to bacterial infections[43,44]. The defect in T-cell-dependent antibody response is, in turn, explained by the inability of BCL-6 null mice to form germinal centers, the main site for Ig isotype switching and affinity maturation. Our results show that although there is a weak primary antigen-specific Ig response with some class switching, no high-affinity antibodies are produced (Fig. 4). This result supports the notion that GCs may be absolutely necessary in this regard, but not for Ig-class switching. The high morbidity of BCL-6 null mice in the presence of low dose bacteria present in a 'barrier' animal facility[45] suggest that these animals may be severely immunodeficient.

BCL-6 as a specific regulator of germinal-centre formation

Based on morphological evidence as well as on the absence of B cells expressing the GC marker PNA, BCL-6 null mice displayed a complete inability to form GC. Variable defects in GC formation have been observed in mice lacking the related receptors CD40 (ref. 46) and type-I TNF receptor[47], or their respective ligands CD40L[48] and lymphotoxin-α[47], as well as in mice lacking the B-cell surface molecule CD19 (ref. 49), the signal transducer Lyn[50], the IkB-type molecule BCL-3 (ref. 51), and the B-cell-specific transcription coactivator OCA-B[52,53]. However, in all these cases the GC defect was part of, and probably secondary to, broader defects in B-cell lineage development (CD19, OCA-B and Lyn), the result a general disturbance in lymphoid organ development (in the mice lacking lymphotoxin-α, type-I TNF receptor or BCL-3), or was only partial, with scattered clusters of cells displaying a typical GC phenotype (in mice lacking CD40$^{-/-}$ and CD40L; unpublished data, C.G.). In contrast, *BCL-6*$^{-/-}$ mice displayed a selective and complete defect in GC formation in the absence of qualitative or quantitative alterations of lymphoid organ or overall B-cell lineage development. This phenotype, together with the specific pattern of expression of BCL-6 in GC B cells[25], suggests that BCL-6 may trigger a signal essential for GC formation. Because BCL-6 downregulates IL-4 signaling (Chang, C.-C., pers. comm.) and is downregulated by CD40 activation[26], it is conceivable that it may play a central role in integrating various signals that regulate GC formation and GC-dependent B-cell-mediated immune responses.

The precise mechanism by which BCL-6 controls GC formation remains to be elucidated. Since BCL-6 is normally expressed in T cells as well as in B cells within GC[25], the lack of GC may be due to inadequate T-cell priming and/or decreased B-cell responsiveness. This question can be addressed by analysing GC formation in chimeric mice obtained by injection of *BCL-6* null ES cells into the blastocysts of mice lacking either the B or T cell lineage[54,55]. Regardless of the cellular components involved, the fact that the B cell expressing the inactive BCL-6 molecule does not acquire PNA and PCNA markers demonstrates that BCL-6 controls both proliferation and differentiation of B cells into GC.

Implications for lymphomagenesis

Our data provide direct insights into the role of BCL-6 in the pathogenesis of DLCL, tumors thought to derive from GC B cells[56]. Of the DLCLs in which BCL-6 function is perturbed, appoximately 30% carry *BCL-6* translocations which deregulate BCL-6 expression by promoter substitution[10]. In most of the remaining fraction of DLCL and in 45% FL, the *BCL-6* promoter region is affected by mutations that, at least in some cases studied, have also been shown to deregulate its expression (our unpublished results. Therefore, in most B-cell lymphomas, the switch off of BCL-6 expression normally associated with exit from GC failed to occur. The observation that BCL-6-deficient B cells fail to form GC because they fail to undergo activation and rapid proliferation, implies that a B cell carrying a deregulated *BCL-6* gene may be altered in these functions. Thus, alterations of BCL-6 expression by chromosomal translocation may contribute to lymphomagenesis by triggering an uncontrolled clonal expansion of the GC precursor cell.

Methods

Targeted Disruption of the *BCL-6* Gene in the Mouse Germline. The murine *BCL-6* genomic locus was cloned from a genomic library constructed from mouse strain 129/Sv DNA using a human *BCL-6* cDNA clone as a probe. The exon-intron organization was determined by restric-

tion endonuclease and DNA sequencing analysis. The first targeting vector was constructed from plasmid pPNT[57] by inserting a 6.5-kb *Eco*RI-*Bgl*II *BCL-6* genomic fragment upstream and a 2.8-kb *Hin*dIII fragment downstream of the pGKNeo cassette which, after homologous recombination, replaces the *BCL-6* exons 8–9 coding four of six BCL-6 zinc-fingers[2] (Fig. 1*a*). The second pPNT-derived targeting construct contained a 2.0-kb *Hin*d III-*Eco*RI fragment containing the BCL-6 exon 3 region and a 6.9-kb *Sac*I fragment downstream of the BCL-6 encoding region. This contruct replaced BCL-6 exons 4–9 as well as the coding region of exon 10 (Fig. 1*b*). The targeting vectors were linearized and electroporated into CJ7 ES cells as described before[58]. G418 and gancyclovir-resistant clones were screened for homologous recombination by Southern blot analysis using diagnostic digestions and probes as shown in Fig. 1. Generation of chimeras and breeding of mutant mice were essentially as described[58]. Genomic DNA was extracted from mouse tail tissue, digested with *Xba*I, and hybridized to the HX1.2 probe shown in Fig. 1*a*, or digested with *Eco*RI and hybridized to the *Sac*II probe shown in Fig. 1*b*.

Histology and immunohistochemistry. Spleen, thymus, lymph nodes (popliteal, axillary, submandibular and mesenteric), liver and Peyer's patches were fixed in 10% buffered formalin overnight at RT and embedded in paraffin. The remaining carcass was fixed as above, decalcified in CalEx (Fisher Diagnostics, FairLawn, NJ), serially sectioned and embedded in paraffin. Four µm-thick, dewaxed and antigen-retrieved (0.001M EDTA pH7.5 for 15 min at 100 C°) paraffin sections were stained for H&E and immunostained[25].

The antibodies used were polyclonal rabbit anti GST-BCL-6 fusion protein (N3; Santa Cruz Biotechnology, Santa Cruz, CA), rabbit (rb) anti-TdT (Sera-Lab), Ki-67 (Novocastra Laboratories), rabbit anti-CD3, myeloperoxidase, lysozyme, S-100, mouse anti-PCNA (PC10) (Dako), goat (gt) anti-mouse IgE, IgD (ICN), IgG1, IgG2a, IgG2b, IgM (Southern Biotechnology Associates), goat anti-peanut lectin (Vector), rat anti-mouse CD45R/B220 (RA3-6B2), CD43 (S7) and syndecan (281-2) (Pharmingen), gt anti mouse IgA, mouse ascites (MOPC21) (Sigma). Biotinylated Arachis Hypogea lectin (PNA) was purchased from Sigma and used at 5 µg/ml. Primary antibodies were counterlabelled with species-specific biotin- or AP-conjugated antibodies. Avidin-AP and -HRP were purchased from Dako. For single colour immunohistochemistry, the antibodies were revealed with peroxidase-conjugated avidin and AEC (Sigma) brown precipitation. Slides stained for BCL-6 were then restained for PNA in two colour immunostaining and developed in AP with Fast Blue (Sigma) diazonium salts[25]. Double and triple stainings were performed with species-specific secondary antibodies conjugated with FITC, TRITC and biotin (Southern Biotechnology Associates; these latter counterstained with Avidin-AMCA, Vector).

Bacterial, parasite and viral diagnostics. Bacterial and parasitic infections were evaluated by morphologic microscopic examination of the lesions, the mucosal surfaces (gastrointestinal tract, respiratory mucosa), and the gastrointestinal tract content. In addition, special stains were employed: Acid Fast (to detect mycobacteria), Gram (to detect Gram+ and Gram– bacteria) and Whartin-Starry silver stain (to detect fusospirillar organisms, CARbacillum, fungi, pneumocystis and helminths). Circulating antibodies against 19 murine viral pathogens were tested by Charles River Laboratories (MA).

Flow cytometry analysis. Spleen, thymus, bone marrow and peritoneal cavity lavage (PerC) were obtained from at least two 4-week-old homozygous mice per ES line and from at least three wild-type and three heterozygous littermates. Single-cell suspensions were prepared and stained using standard procedures, with appropriate combinations of fluorochrome and/or biotin-labelled monoclonal antibodies, and analysed on a five-colour FACStar Plus flow cytometer (Beckton-Dickinson) with PI exclusion of dead cells as previously described[60]. Fluorochrome-conjugated antibodies for flow cytometry were: FITC-anti-IgM (331.12), biotin-anti-IgD (AF6-122.2), FITC- or APC-anti B220 (RA3-6B2), biotin-anti-CD23 (B3B4), PE-anti-CD43 (S7), APC-anti-Mac-1 (M1/70), APC-anti-CD5 (53.7.8), biotin-anti-CD3 (2C11), APC-anti-CD4 (GK1.5) and FITC-anti-CD8 (53.7). Antibodies to CD23, CD3 and CD43 were purchased from PharMingen (San Diego). All other antibodies were purified and conjugated as previously described[61].

Immunization and ELISA. The mice used in the anti-NP response studies were the progeny of (B6x129)F2 inter-crosses. Both the 129 and B6 strains carry the IgH-C/Vb haplotype and are good responders to NP-conjugates. 11-week-old mice were immunized intraperitoneally with NP_{20}-KLH (100 µg per mouse) in complete Freund's adjuvant (CFA). Eleven days later, all immunized animals were bled and sacrificed and their spleens removed for immunohistochemical and ELISA analyses. For reconstituted RAG-1 mice, 12-week-old animals were immunized intraperitoneally with 1×10^5 SRBCs in PBS and sacrificed 11 days later for analysis. Resting-level serum immunoglobulins were measured by sandwich ELISA using unlabelled anti-mouse Ig antibodies as capture reagent, AP-labelled anti-mouse Ig subclass-specific antibodies as developing reagents (Southern Biotechnology Associates) and 4-methyl umbelliferyl phosphate (Sigma, St Louis, MO) as AP substrate. Serum values were measured against control mouse Ig isotype standards. NP-specific serum antibodies were measured similarly except that NP_{14}-BSA was used as plate coat and the relative titre of NP-specific antibodies are expressed as the relative of dilutions that gave fluorescence counts within linear range of the assay.

Measurement of affinity maturation. Mice were immunized intraperitoneally with 100 µg NP_{20}-KLH in CFA on day 0 and bled on day 5. On days 21 and 42, the mice were boosted with 10 µg NP_{20}-KLH in incomplete Freund adjuvant and bled 5 days after each immunization. NP-specific IgG1 antibodies of high and low affinities were assayed by their relative binding to NP_3-BSA- and NP_{23}-BSA- coated plates[62]. Low-affinity antibodies will bind to the highly haptenated protein (NP_{23}-BSA), but not to the lightly haptenated protein (NP_3-BSA), while high-affinity antibodies bind equally to both the high and low haptenated proteins. Thus, the ratio of binding to NP_3-BSA and NP_{23}-BSA is a measure of relative avidity of the anti-NP antibodies. Each antiserum was titrated on both NP_3-BSA and NP_{23}-BSA coated plates. The NP_3/NP_{23}-BSA ratio is calculated as the ratio of the amount of antibody (1/serum dilution) required to give equal binding (fluorescence counts) on each protein-coated plate.

***RAG-1*$^{-/-}$ complementation assay.** *BCL-6*$^{+/\Delta}$ ES cells generated by homologous recombination were subjected to selection with increased neomycin concentration[59] and the resistant clones were screened for *BCL-6* status by Southern blot analysis. *BCL-6*$^{\Delta/\Delta}$ ES cells derived from two distinct *BCL-6*$^{+/\Delta}$ clones were injected into *RAG-1*$^{-/-}$ blastocysts (Jackson Laboratories). The resulting chimaeric mice were screened for ES cell-reconstitution by both Southern blot analysis of tail DNA and CD3 staining of circulating T cells (data not shown). Passage-matched *BCL-6*$^{+/+}$ ES cells were also injected as a positive control for lymphoid reconstitution. To analyse GC formation, 6 *BCL-6*$^{\Delta/\Delta}$/*RAG-1*$^{-/-}$ chimaeric animals (derived from 2 *BCL-6*$^{+/\Delta}$ ES clones) and 3 control (*BCL-6*$^{+/+}$/*RAG-1*$^{-/-}$) chimaeras were immunized intraperitoneally with 1 X 10^5 SRBCs in PBS and sacrificed 11 days later for analysis.

Acknowledgements

The authors are grateful to E. Marcantonio for critical reading of the manuscript, to V. Soares for help with blastocyst injections and to S.R. Brunnert for consultation on the histopathologic data. B.H.Y. is a Leukemia Society of America Fellow, G.C. is a Leukemia Society of America Special Fellow and A.M.S. and P.R. are Leukemia Society of America Scholars.

Received 12 March; accepted 2 May 1997.

1. Ye, B.H., Rao, P.H., Chaganti, R.S.K. & Dalla-Favera, R. Cloning of bcl-6, the locus involved in chromosomal translocations affecting band 3q27 in B-cell lymphoma. *Cancer Res.* **53**, 2732–2735 (1993).
2. Ye, B.H. *et al.* Alterations of a zinc-finger encoding gene, *BCL-6,* in diffuse large-cell lymphoma. *Science* **262**, 747–750 (1993).
3. Baron, B.W. *et al.* Identification of the gene associated with the recurring chromosomal translocations t(3;14)(q27;q32) and t(3;22)(q27;q11) in B-cell lymphomas. *Proc. Natl. Acad. Sci. USA* **90**, 5262–5266 (1993).
4. Deweindt, C. *et al.* Cloning of a breakpoint cluster region at band 3q27 involved in human non-Hodgkin's lymphoma. *Genes Chromosomes Cancer* **8**, 149–154 (1993).
5. Kerckaert, J.-P. *et al. LAZ3*, a novel zinc-finger encoding gene, is disrupted by recurring chromosome 3q27 translocations in human lymphoma. *Nature Genet.* **5**, 66–70 (1993).
6. Miki, T., Kawamata, N., Hirosawa, S. & Aoki, N. Gene involved in the 3q27 translocation associated with B-cell lymphoma, *BCL5,* encodes a Krüppel-like zinc-finger protein. *Blood* **83**, 26–32 (1994).
7. Lo Coco, F. *et al.* Rearrangements of the BCL-6 gene in diffuse large-cell non-Hodgkin lymphoma. *Blood* **83**, 1757–1759 (1994).
8. Bastard, C. *et al. LAZ3* rearrangements in non-Hodgkin's lymphoma: Correlation with histology, immunophenotype, karyotype, and clinical outcome in 217 patients. *Blood* **83**, 2423–2427 (1994).
9. Otsuki, T. *et al.* Analysis of LAZ3 (BCL-6) status in B-cell non-Hodgkin's lymphomas: Results of rearrangement and gene expression studies and a mutational analysis of coding region sequences. *Blood* **85**, 2877–2884 (1995).
10. Ye, B.H. *et al.* Chromosomal translocations cause deregulated BCL6 expression by promoter substitution in B cell lymphoma. *EMBO J.* **14**, 6209–6217 (1995).
11. Migliazza, A. *et al.* Frequent somatic hypermutation of the 5' non-coding region of the BCL-6 gene in B-cell lymphoma. *Proc. Natl. Acad. Sci. USA* **92**, 12520–12524 (1995).
12. Gaidano, G., *et al.* Frequent mutation of the 5' non-coding region of the BCL-6 gene in AIDS-related non-Hodgkin's lymphomas. *Blood* (in the press).
13. Dalla-Favera, R. *et al.* BCL-6 in diffuse large-cell lymphomas. In: *Important Advances in Oncology 1996.* (eds DeVita, V. T., Hellman, S. & Rosenberg, S.A.) 139–148 (Lippincott, Philadelphia, 1996).
14. Chang C.-C., Ye, B.H, Chaganti, R.S.K. & Dalla-Favera, R. BCL-6, a POZ/Zinc-finger protein, is a sequence specific transcription repressor. *Proc. Natl. Acad. Sci. USA* **93**, 6947–6952 (1996).
15. Seyfert, V.L., Allman, D., He, Y. & Staudt, L.M. Transcriptional repression by the proto-oncogene BCL-6. *Oncogene* **12**, 2331–2342 (1996).
16. Albagli, O., Dhordain, P., Deweindt, C., Lecocq, G. & Leprince, D. The BTB/POZ domain: a new protein-protein interaction motif common to DNA- and actin-binding proteins. *Cell Growth & Differ.* **6**, 1193–1197 (1995).
17. Harrison, S.D. & Travers, A.A. The *Tramtrack* gene encodes a *Drosophila* finger protein that interacts with the *ftz* transcriptional regulatory region and shows a novel embryonic expression pattern. *EMBO J.* **9**, 207–216 (1990).
18. DiBello, P.R., Withers, D.A., Bayer, C.A., Fristrom, J.W., & Guild, G.M. The *Drosophila Broad-Complex* encodes a family of related proteins containing zinc fingers. *Genetics* **129**, 385–397 (1991).
19. Chardin, P., Courtois, G., Mattei, M.G., & Gisselbrecht, S. The *KUP* gene, located on human chromosome 14, encodes a protein with two distant zinc fingers. *Nucleic Acid Res.* **19**, 1431–1436 (1991).
20. Bardwell, V. J. & Treisman, R. The POZ domain: a conserved protein-protein interation motif. *Genes & Dev.* **8**, 1664–1677 (1994).
21. Chen, Z. *et al.* Fusion between a novel Krüppel-like zinc finger gene and the retinoic acid receptor-α locus due to a variant t(11;17) translocation associated with acute promyelocytic leukemia. *EMBO J.* **12**, 1161–1167 (1993).
22. Koonin, E.V., Senkevich, T.G., & Chernos, V.I. A family of DNA virus genes that consists of fused portions of unrelated cellular genes. *Trends Biochem. Sci.* **17**, 213–214 (1992).
23. Xue, F. & Cooley, L. *Kelch* encodes a component of intercellular bridges in *Drosophila* egg chamber. *Cell* **72**, 681–693 (1993).
24. Deweindt, C. *et al.* The LAZ3/BCL6 oncogene encodes a sequence-specific transcriptional inhibitor: a novel function for the BTB/POZ domain as an autonomous repressing domain. *Cell Growth Differ.* **6**, 1495–1503 (1995).
25. Cattoretti, G. *et al.* The BCL-6 protein is expressed in germinal centre B-cells. *Blood* **86**, 45–53 (1995).
26. Allman, D. *et al.* BCL-6 expression during B-cell activation. *Blood* **87**, 5257–5268 (1996).
27. Onizuka, T. *et al.* BCL-6 gene product, a 92-98-kD nuclear phosphoprotein, is highly expressed in germinal centre B cells and their neoplastic counterparts. *Blood* **86**, 28–37 (1995).
28. Flenghi, L. *et al.* Monoclonal antibodies PG-B6a and PG-B6p recognize, respectively, a highly conserved and a formol-resistant epitope on the human BCL-6 protein amino-terminal region. *Am. J. Pathol.* **148**, 1543–1555 (1996).
29. Dhordain, P. *et al.* The BTB/POZ domain targets the LAZ3/BCL6 oncoprotein to nuclear dots and mediates homomerisation *in vivo*. *Oncogene* **11**, 2689–2697 (1995).
30. Murray, A.B. & Luz, A. Acidophilic macrophage pneumonia in laboratory mice. *Vet. Pathol.* **27**, 274–281 (1990).
31. Abbas, A.K., Murphy, K.M. & Sher, A. Functional diversity of helper T lymphoctes. *Nature* **383**, 787–793 (1996).
32. Hardy, R.R. & Hayakawa, K. B-lineage differentiation stages resolved by multiparameter flow cytometry. *Ann. N.Y. Acad. Sci. USA* **764**, 19–24 (1995).
33. Wells, S.M., Kantor, A.B., & Stall, A.M. CD43 (S7) expression identifies peripheral B cell subsets. *J. Immunol.* **153**, 5503–5515 (1994).
34. Liu, Y.J., Johnson, G.D., Gordon, J. & MacLennan, I.C. Germinal centres in T-cell-dependent antibody responses. *Immunol. Today* **13**, 17–21 (1992).
35. Küppers, R., Zhao, M., Hansmann, M.-L., & Rajewsky, K. Tracing B cell development in human germinal centres by molecular analysis of single cells picked from histological sections. *EMBO J.* **12**, 4955–4967 (1993).
36. Rose, M.L. Birbeck, M.S., Wallis, V.J., Forrester, J. A. & Davies, A. J. Peanut letin binding properties of germinal centres of mouse lymphoid tussue. *Nature* **284**, 364–366 (1980).
37. Orazi, A., Du, X., Yang, Z., Kashai, M. & Williams, D.A. Interleukin-11 prevents apoptosis and accelerates recovery of small intestinal mucosa in mice treated with combined chemotherapy and radiation. *Lab. Invest.* **75**, 33–42 (1996).
38. Mombaerts, P. *et al.* RAG-1-dificient mice have no mature B and T lymphocytes. *Cell* **68**, 869–877 (1992).
39. Snapper, C.M., Finkelman, F.D. & Paul W.E. Regulation of IgG1 and IgE production by interleukin 4. *Immunol. Rev.* **102**, 51–75 (1988).
40. Del Prete, G. *et al.* IL-4 is an essential factor for the IgE synthesis induced *in vitro* by human T cell clones and their supernatants. *J. Immunol.* **140**, 4193–4198 (1988).
41. Koike, M. & Takatsu, Y. IL-5 and its receptor: which role do they play in the immune response? *Int. Arch. Allergy Immunol.* **104**, 1–9 (1994).
42. Mosmann, T.R. & Coffman, R.L. Th1 and Th2 cells: Different patterns of lymphokine secretion lead to different functional properties. *Annu. Rev. Immunol.* **7**, 145–173 (1989).
43. Hong, R. Diseases due to immunologic deficiency. In: *Nelson Textbook of Pediatrics.* Edn.13, (eds Behrman, R.E., Vaughan III, V.C. & Nelson, W.E.) 461–466 (W.B. Saunders Company, Philadelphia, 1987).
44. Ishizaka, A. *et al.* Regulation of IgE and IgG4 synthesis in patients with hyper IgE syndrome. *Immunol.* **70**, 414–416 (1990).
45. Crabbe, P.A., Nash, D.R., Bazin, H., Eyssen, H. & Heremans, J.F. Immunohistochemical observations on lymphoid tissues from conventional and germ-free mice. *Lab. Invest.* **22**, 448–452 (1970).
46. Kawabe, T. *et al.* The immune responses in CD40-deficient mice: impaired immunoglobulin class switching and germinal centre formation. *Immunity* **1**, 167–178 (1994).
47. Matsumoto, M. *et al.* Role of lymphotoxin and the type I TNF receptor in the formation of germinal centers. *Science* **271**, 1289–1291 (1996).
48. Renshaw, B. R. *et al.* Humoral immune responses in CD40 ligand-dificient mice. *J. Exp. Med.* **180**, 1889–1900 (1994).
49. Rickert, R.C., Rajewsky, K. & Roes, J. Impairment of T-cell-dependent B-cell response and B-1 cell development in CD19-deficient mice. *Nature* **376**, 352–376 (1995).
50. Hibbs, M. L. *et al.* Multiple defects in the immune system of *Lyn*-deficient mice, culminating in autoimmune disease. *Cell* **83**, 301–311 (1995).
51. Schwarz, E.M., Krimpenfort, P., Berns, A. & Verma, I.M. Immunological defects in mice with a targeted disruption in Bcl-3. *Genes & Dev.* **11**, 187–197 (1997).
52. Schubart, D.B., Rolink, A., Kosco-Vilbois, M.H., Botteri, F. & Matthias, P. B-cell-specific coactivator OBF-1/OCA-B/Bob1 required for immune response and germinal centre formation. *Nature* **383**, 538–542 (1996).
53. Kim, U. *et al.* The B-cell-specific transcription coactivator OCA-B/OBF-1/Bob-1 is essential for normal production of immunoglobulin isotypes. *Nature* **383**, 542–547 (1996).
54. Kitamura, D., Roes, J., Kuhn, R. & Rajewsky, K. A B cell-deficient mouse by targeted disruption of the membrane exon of the immunoglobulin mu chain gene. *Nature* **350**, 423–426 (1991).
55. Mombaerts, P. Lymphocyte development and function in T-cell receptor and RAG-1 mutant mice. *Int. Rev. Immunol.* **13**, 43–63 (1995).
56. Stein, H. & Dallenbach, F. Diffuse large cell lymphomas of B and T cell type. In: *Neoplastic hematopathology.* (ed. Knowles, D.M.) 675–714 (Williams & Wilkins, Baltimore, 1992).
57. Tybulewicz, V.L., Crawford, C.E., Jackson., P.K., Bronson, R.T. & Mulligan, R.C. Neonatal lethality and lymphopenia in mice with a homozyous disruption of the c-abl proto-oncogene. *Cell* **65**, 1153–1163 (1991).
58. Swiatek, P.J. & Gridley, T. Perinatal lethality and defects in hindbrain development in mice homozygous for a targeted mutation of the zinc finger gene Krox20. *Genes Dev.* **7**, 2071–2084 (1993).
59. Mortensen, R.M., Conner, D.A., Chao, S., Geisterfer-Lowrance, A.A.T. & Seidman, J.G. Production of homozygous mutant ES cells with a single targeting construct. *Mol. Cell. Biol.* **12**, 2391–2395 (1992).
60. Stall, A.M. & Wells, S.M. FACS analysis of murine B cell populations. In: *The Handbook of Experimental Immunology,* Edn. 5. (eds Weir, D.M., Herzenberg, L.A., Blackwell, C.C. & Herzenberg, L.A.) Vol. 2, Chapter 63 (Blackwell, Edinburgh, 1997).
61. Lam, K.-P. & Stall, A. M. Major histocompatability complex class II expression distinguishes two distinct B cell developmental pathways during ontogeny. *J. Exp. Med.* **180**, 507–517 (1994).
62. Roes, J. & Rajewsky, K. Bcl-2 increases memory B cell recruitment but does not perturb selection in germinal centers. *J. Exp. Med.* **177**, 45–55 (1993).
63. Luna, L.G. *Manual of Histologic Staining Methods* (MacGraw-Hill, New York, 1960).